Lifetime maximum load effects on short-span bridges subject to growing traffic volumes

E.J. OBrien[1], A. Bordallo-Ruiz[1,2] and B. Enright[3]

[1] School of Civil, Structural and Environmental Engineering, University College Dublin, Ireland
[2] AERTEC Solutions, Málaga, Spain
[3] Department of Civil and Structural Engineering, Dublin Institute of Technology, Ireland

Keywords: Bridge, traffic loading, non-stationary, time-dependent, characteristic, growth.

Abstract
This paper investigates the phenomenon of growth in truck volumes during the lifetime of a bridge and the influence of that growth on characteristic maximum load effects. The study uses Weigh-in-Motion (WIM) data from the Netherlands to calibrate Monte Carlo simulation of load effects on a range of bridge spans. For short spans, the distribution of 25-day maximum data is Weibull. As span increases, a better fit is obtained with a mixture that separates low loader vehicles from all others. Growth is addressed by assuming constant, linear or quadratic variations in the properties of the best-fit Generalized Extreme Value distributions. The principle of parsimony is used to select the most appropriate fit. Growth is shown to change the nature of the trend on probability paper, shifting the curves to the right. While the influence of growth is relatively modest, fitting non-stationary data to a stationary curve gives erroneous results.

1. Introduction

As the existing stock of bridges ages, there is an increasing need for the assessment and maintenance of these structures. Load, and resistance to it, are equally important inputs into a bridge safety assessment. This paper considers the process of finding site-specific characteristic load effects using measured traffic data, i.e., it considers the loading side of the load/resistance inequality. In particular, it addresses the issue of traffic growth and its implications for bridge safety.

Traffic loading is perhaps the most variable input in any calculation of the reliability of a bridge [1]. In the literature on traffic load effect estimation, effects have been found from directly measured traffic, usually captured used Weigh-in-Motion (WIM) technologies, or Monte Carlo simulations calibrated using WIM data. Various methods of extrapolation have been used, including the fitting of statistical distributions to the resulting histograms of measured traffic [2,3], the use of parent distributions [4,5], Rice's formula developing an optimal threshold level [3,6], the use of a distribution of block maxima [7,8,9] or the use the peaks over threshold (POT) extreme value approach [10,11].

Data is generally filtered and only the block maximum retained. The block length should be selected to remove natural variations. For example, a block length of one day removes the influence of peak truck traffic flow periods during the 24 hour period. Cooper [12,13] used this

strategy, terming it the 'homogenous day'. A daily maximum approach was also adopted by Moyo et al. [14] when fitting recorded strain measurements on a bridge to Gumbel probability paper.

Caprani et al. [15] recognize that traffic loading events are a mixture of different forms and therefore should be represented by a mixture of distributions. They use this approach to find characteristic traffic load effects on short to medium span (20-50 m) bridges. Two lane, bidirectional bridges in this span range, are governed by free flowing traffic [2]. More recently, OBrien and Enright [16] have combined extreme value theory (EVT) with Monte Carlo simulations in order to simulate thousands of years of traffic, reducing the uncertainty associated with extrapolation and identifying the typical loading scenarios which produce lifetime maximum load effects. Despite all these research efforts, there is almost no literature on non-stationary traffic analysis.

As economies grow, road freight volumes tend to grow (Figure 1). Despite the recent economic downturn, the European Commission predicts a sustainable annual growth in road freight volume of between 1.5% and 2% per annum until 2030 [17].

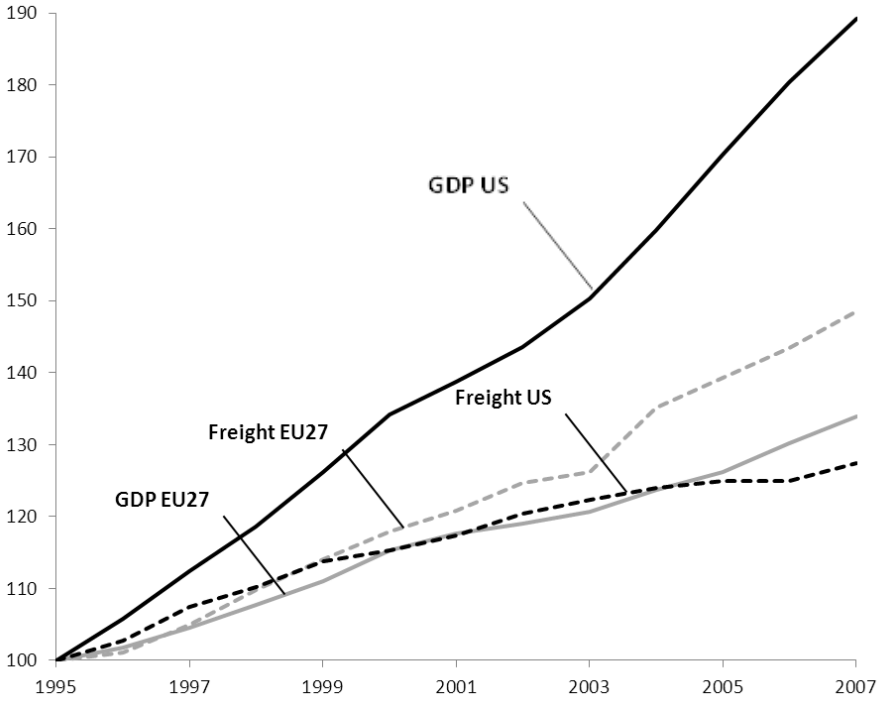

Figure 1: Road Freight and Gross Domestic Product (GDP) indexes for US (US Department of Transport) and EU27 (European Commission) using the year 1995 as a reference (1995=100).

Most calculations of characteristic load effect [15,16] assume stationary conditions of traffic. Indeed, three mechanisms of growth could be envisaged to justify the road freight growth

depicted in figure 1: i) growth in the weights of the vehicles, ii) growth in the numbers of vehicles during the bridge design life or iii) a combination of the two. While the former is related to changes in policies and therefore, does not fall within the scope of this paper, the latter is related to increases in traffic density and represents the core of the present paper. Only a few examples of non-stationary assumptions exist in the literature. Fu and Hag-Elsafi [8] account for the influence of traffic non-stationarity in the assessment of existing structures, focusing on growth in overloaded vehicles and their frequency of occurrence.

The two main methods for the calculation of characteristic load effects [18], are the block maxima and peaks over threshold (POT) approaches. Non-stationary techniques, using both methodologies, are widely used in other fields to estimate extreme effects. Examples of their application are to be found in oceanographic engineering as described by Mendez et al. [19] where monthly extreme sea levels are analysed using a non-stationary Generalized Extreme Value (GEV) model. Menendez et al. [20] consider the influence of seasonality on their estimate of maximum wave height. Stefanakos and Athanassoulis [21] make use of a non-stationary application of the POT method to determine extreme values of wave heights. Non-stationary approaches are also used in weather science. For example, Ribereau et al. [22] extend the Probability Weighted Moments method to provide accurate GEV-based return levels of daily maximum rainfall. Felici et al. [23] model the mid-latitude atmospheric jet stream using a time-dependent GEV distribution approach. Nadarajah [24] applies the same approach to estimate daily maximum rainfall. Nogaj et al. [25] propose a non-stationary POT approach to estimate climatic variables while Renard et al. [26] use the same approach to determine characteristic extreme values for river flows in streams. In the field of athletic performance fraud, Einmahl and Magnus [27] scrutinize time dependent athletic world records to determine ultimate performance. Finally, in finance, Malevergne et al. [28] show the inefficiency of the use of GEV and Generalized Pareto Distribution to estimate empirical distributions of stock returns. In another example, Wang et al. [29] use de-clustering of time-dependent data to estimate value-at-risk levels on security investments.

2. Extreme Value Statistics of a Non-Stationary Process

2.1 Stationary Traffic Models

Extreme value theory provides a framework for the estimation of characteristic load effects for bridges. A common approach to working with extreme value data is to group the data into blocks of equal duration and fit a curve to the maximum of each block. If the blocks are very large, the block maximum data will converge towards one of the Extreme Value family of distributions. The choice of block size is important as blocks that are too small may result in data that has not yet converged to an Extreme Value distribution and blocks that are too large generate too few block maxima, which leads to estimation variance. Block maximum data is often fitted to the Generalized Extreme Value (GEV) distribution which is a general form that encompasses the Gumbel, Weibull and Fréchet distributions. For example, the maximum load effect in one year, M_n, is the maximum of many daily maximum load effects, X_i.

$$M_n = \max\{X_1, \ldots, X_n\} \quad (1)$$

where X_1, ... , X_n, is a sequence of independent random variables having a common distribution function F. In theory the distribution of M_n can be derived exactly for all values of n:

$$\Pr(M_n \le x) = \Pr(X_1 \le x) \times \Pr(X_2 \le x) \times \Pr(X_3 \le x) \ldots\ldots = F(x)^n \ldots\ldots \quad (2)$$

Unfortunately, most of the times, the distribution function $F(x)$ is unknown, and therefore, equation (2) is of little use. However, it is possible to analyze the behavior of $F(x)^n$ when $n \to \infty$. In order to avoid degeneration of the variable M_n (Coles [18]), it has to be linearly normalized, as follows

$$M_n^* = \frac{M_n - b_n}{a_n} \quad (3)$$

for sequences of constants $\{a_n>0\}$ and $\{b_n\}$ that stabilize the location and scale of M^*_n as n increases, avoiding the difficulties that arise with the variable M_n. By the extremal types theorem, given that there exist sequences of constants $\{a_n>0\}$ and $\{b_n\}$ such that

$$\Pr((M_n - b_n)/a_n \le x) \to G(x) \qquad as\ n \to \infty \quad (4)$$

where G is a non-degenerate distribution function, then the GEV distribution is the limit distribution of properly normalized maxima of a sequence of independent and identically distributed (iid) random variables. Because of this, the GEV distribution is used as an approximation to model the maxima of long (finite) sequences of random variables [30,31]. The cumulative distribution function (cdf) is given by:

$$Z_t \sim GEV(\mu, \sigma, \xi) = G(x; \theta) = \exp\left\{ -\left[1 - \xi\left(\frac{x - \mu}{\sigma} \right) \right]_+^{\frac{1}{\xi}} \right\} \quad (5)$$

where t represents time and, for large t, Z_t converges to the Generalized Extreme Value distribution (GEV) with parameter vector $\theta = (\mu, \sigma, \xi)^T$. The parameters describing the distribution are the location, μ, the scale, σ and the shape parameter, ξ. The value of the shape parameter determines which distribution of the Extreme Value family is described by Equation (5). For $\xi = 0$, it is the Gumbel distribution, for $\xi > 0$, it is the Fréchet or type II Extreme Value distribution and for $\xi < 0$, it is the Weibull or type III distribution. The extremal type theorem implies that, when M_n can be stabilized with suitable sequences $\{a_n\}$ and $\{b_n\}$, the corresponding normalized variable M^*_n has a limiting distribution that must be one of the three types of extreme value distribution which are the only possible limits for the distributions of M^*_n. The combination of $\{a_n\}$ and $\{b_n\}$, determines which of the three types of distribution will be the limiting distribution. Therefore it is common to refer to the domains of attraction of the Fréchet, Gumbel and Weibull distributions,

2.2 The non-stationary GEV distribution

A block is considered that is sufficiently small (e.g., 1 day) so that growth during the period of the block can be neglected. The probability of the block maximum, *X*, not exceeding a level, *x*, is given by the cdf:

$$Z_i = \Pr(X \le x) = F_i(x) \tag{6}$$

Growth is then considered between blocks which changes the parent distributions, F_i. The probability of non-exceedance in a lifetime of *n* blocks is:

$$Z_t = \Pr(X_1 \le x) \times \Pr(X_2 \le x) \times \Pr(X_3 \le x) \ldots\ldots = F_1(x) \times F_2(x) \times F_3(x) \ldots\ldots \tag{7}$$

Hence, for *n* blocks,

$$Z_t = \prod_{i=1}^{t} F_i(x) \tag{8}$$

It is usual to adopt a pragmatic approach of using the standard extreme value models as basic templates that can be enhanced by statistical modeling (Coles [18]). Assuming this, maximum likelihood estimation (MLE) techniques can be expanded to cater for traffic growth. It is then possible to define a non-stationary family of GEV distributions (nsGEV), with parameters no longer constant in time.

$$Z_t \sim \mathrm{GEV}(\mu(t), \sigma(t), \xi(t)) = G(x; \theta(t)) = \begin{cases} \exp\left\{ -\left[1 - \xi(t)\left(\dfrac{x - \mu(t)}{\sigma(t)} \right) \right]_+^{\frac{1}{\xi(t)}} \right\} & \xi(t) \neq 0 \\ \exp\left\{ -\exp\left[\left(\dfrac{x - \mu(t)}{\sigma(t)} \right) \right] \right\} & \xi(t) = 0 \end{cases} \tag{9}$$

where, now, the parameter vector $\theta(t)=(\mu(t), \sigma(t), \xi(t))$, depends on time.

The effect of changing Z_i can be seen in the following simplified example. A 100 year lifetime is considered with 250 working days per year, i.e. a total lifetime of 25,000 days. A daily growth in the number of trucks of 0.016% is assumed (4.1 % per annum). The block length is taken as 1 day and the truck weights are taken to be normally distributed, with $W_i \sim N(50,5)$, in tonnes. Growth in the number of trucks per day is assumed so the size of the sample from which the maximum is identified each day, increases as the days go by. In order to accurately estimate characteristic maximum GVW with blocks of increasing size, a non-stationary GEV (nsGEV) approach has to be adopted. For such an approach, a family of stationary GEV distributions is fitted to the daily maximum GVW sample (refer to Figure 2). On the first day, there are 1000 trucks and the maximum distribution can be seen to have a mode of about 66 tonnes.

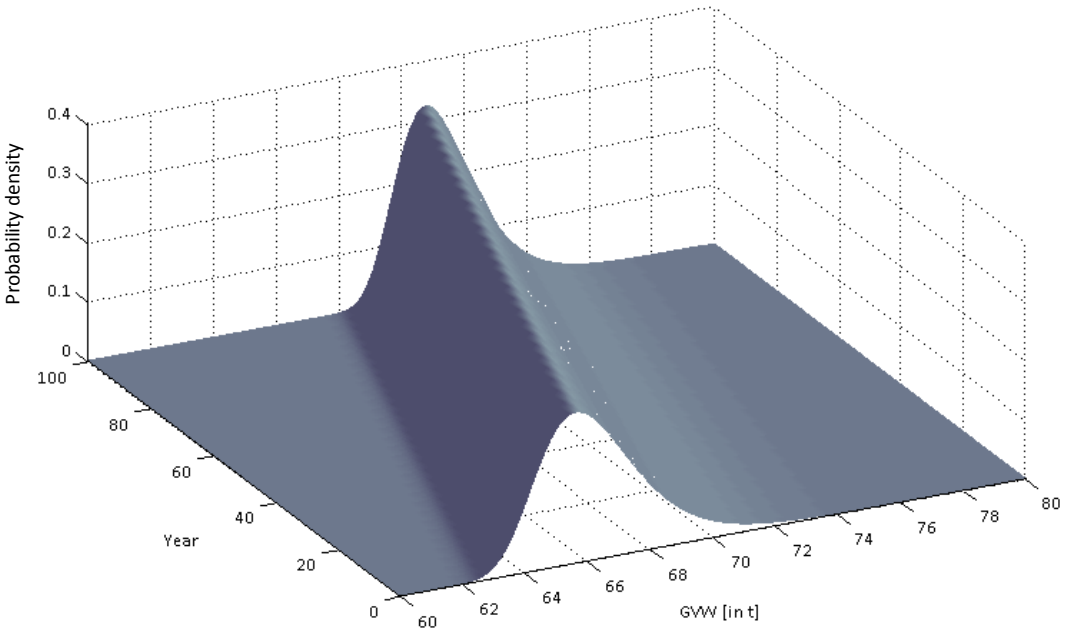

Figure 2: Non-stationary family of GEV distributions obtained to model maximum GVW from daily populations of increasing size

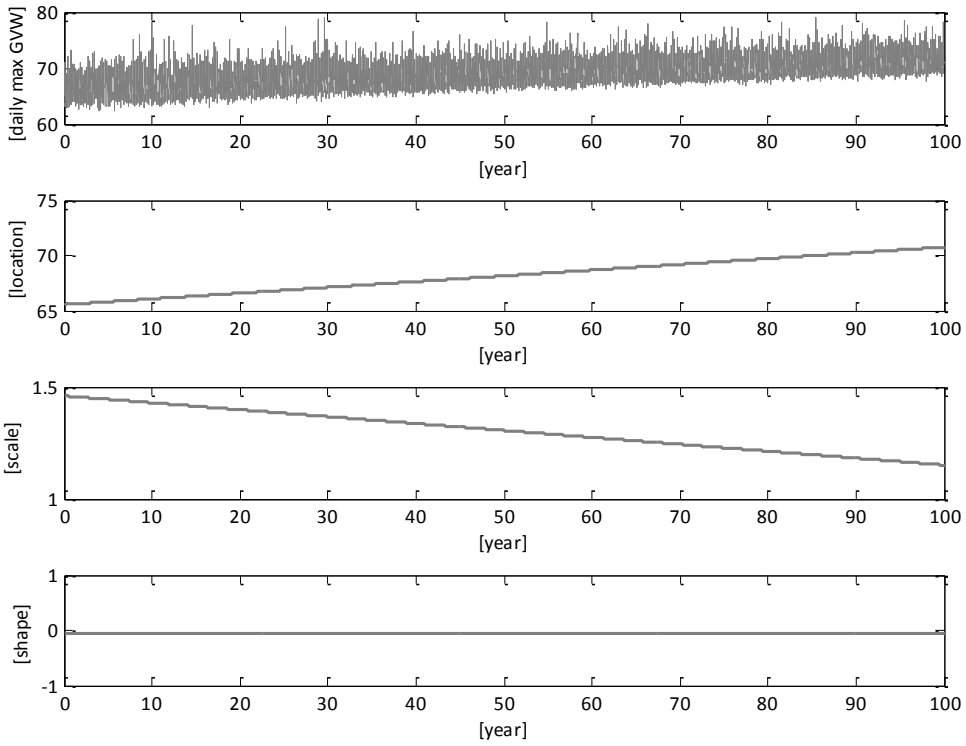

Figure 3: Effect of growth on: i) Non-stationary daily maximum GVW sample, ii) location parameter, iii) scale parameter and, iv) shape parameter for each of the 25,000 GEV fits depicted in Figure 2

As the model is parametrically defined in this example, location, shape and scale parameters for each of the stationary GEV distributions, that conform to the non-stationary model, can be plotted against time – Figure 3. The location parameter increases as the scale parameter decreases. The shape parameter does not change significantly.

Figure 4 illustrates the results on Gumbel probability paper. The black points represent the block maxima where the numbers per block are increasing. The gray points, provided for reference, are block maxima where no growth occurs. For a given level of GVW, the non-stationary probability of exceedance is found by adding the weighted probabilities of exceedance for each day through the lifetime. If a stationary distribution is fitted to non-stationary data (black points), there is a poor fit as the true nature of the underlying distribution is not being reflected in the fitted curve.

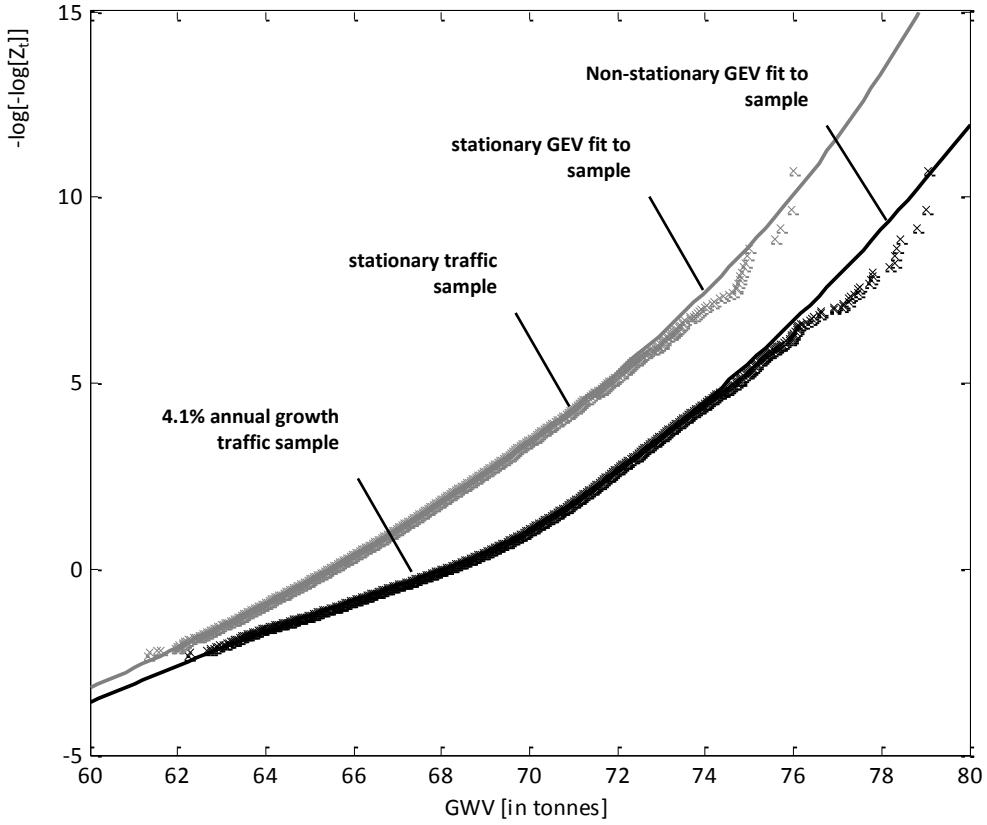

Figure 4: Probability paper plot of daily maximum GVW (in tonnes) for stationary and non-stationary conditions with best-fit stationary and non-stationary distributions.

Non-stationary fits represent the total probability of exceedance beyond a specified level, over a given lifetime. Therefore, in figure 4, the black curve represents the total probability of exceedance of any given GVW in the 100-year lifetime considered in the analysis. It is important to distinguish between 'lifetime', throughout which growth is assumed and return period which

is the average recurrence interval over an extended period of time and can be viewed as an approximate frequency of occurrence. The figure can be used to find characteristic values of GVW for a range of different return periods. However, it is only valid for one lifetime and changing the lifetime changes the whole curve. After an initial shift of the non-stationary trend to the right, the two curves follow a 'parallel' trend, with the non-stationarity causing a modest increase in GVW for a given return period.

3. Influence of growth on Lifetime Maximum Load effects

Statistical distributions derived from WIM measurements are commonly used as the basis for Monte Carlo simulation of traffic loading, and characteristic maximum bridge load effects are estimated by extrapolation from the results of this simulation. Results are highly sensitive to the assumptions made, not just with regard to gross weights but also to such parameters as the number of axles per vehicle and the gaps between axles. The details for each vehicle, and for the spacing between vehicles in each lane, are generated using lane-specific statistical distributions derived from the traffic measured at each site.

In this paper, simulations calibrated against WIM data collected at one European site, near Woerden in the Netherlands in 2005, are used to perform the simulations. The model allows for the simulation of vehicles that are heavier and have more axles than those recorded in the WIM data, and uses techniques for modeling axle configuration that can be applied to any class/type of vehicle. The site is situated on the A12 (E25/E30), with 3 lanes of traffic in one direction of which 2 lanes were monitored with WIM sensors. A total of 646 548 trucks were used to calibrate the simulation, recorded between 7th February and 26th June, 2005 (a total of 20 weeks). The maximum number of axles recorded in the period was 13.

In this study, the GVW and number of axles for each truck are generated using a 'semi-parametric' approach [32]. Up to a certain GVW threshold, where there are enough data to provide a clear frequency trend, an empirical bivariate distribution is used for GVW and number of axles. Beyond this threshold, a parametric fit is needed in order to smooth the trend and so that simulations can generate vehicles with weights and numbers of axles greater than those observed. The tail of a bivariate Normal distribution is fitted to the frequencies above the GVW threshold using truncated maximum likelihood estimation.

OBrien and Enright [16] give details of the approach used to model axle spacing for each vehicle class. For each vehicle measured, all axle spacings are ranked in descending order, starting with the maximum. An empirical distribution is used to generate the maximum axle spacing for each vehicle, given the number of axles and the GVW range (discretized in 5 t intervals). For all spacings other than the maximum, fitted trimodal Normal distributions are used. The *position* of each of the ranked spacings of the vehicle is also modeled in the simulation using empirical distributions for all spacings in each vehicle class.

The proportion of the GVW carried by each individual axle is simulated using bimodal Normal distributions (mixture of two Normal distributions) fitted to the observed data for each axle from each vehicle class. The measured weights of adjacent axles are highly correlated, while the

weights of non-adjacent axles show lower levels of correlation. The observed correlation structure for both adjacent and non-adjacent axles for each vehicle class is achieved in the simulation using the technique of Iman and Conover [33].

The model used here generates vehicles that may have more axles than any observed vehicle. The determination of the axle spacing and loading for these is based on extrapolation from WIM data where the maximum number of axles observed for any vehicle is 13. The magnitude and position of all axle spacings for extrapolated vehicle classes are modeled using trimodal Normal distributions (mixture of three Normal distributions) fitted to measurements for trucks with nine or more axles. Axle loading is modeled using a Normal distribution for each axle, based on the average distribution of axle loads for trucks with nine or more axles. To allow for the varying number of axles in the observed data (i.e., from 9 to 13), the random variable used for each axle is the proportion of the GVW carried by that axle divided by the average weight per axle. The proportion of the GVW carried by each of the front four axles tends to show the greatest variability, with the axles to the rear carrying similar loads.

OBrien and Caprani [34] describe the many approaches used in other studies for modeling headways (the time between the front axles of successive vehicles arriving at the same point on the road). Distributions that have been used include the negative exponential, uniform, gamma, and lognormal, while some authors have used deterministic gaps (e.g., 5 m for congested traffic). Driver behavior is influenced by the clear gap (bumper to bumper) in front of the vehicle. It is not possible to calculate this clear gap from the available WIM data, but it is possible to calculate the inter-axle gap – the gap between the rear axle of the leading truck and the front axle of the following truck. Although headway has been used in other studies, inter-axle gap is used here as it is a better proxy for the clear gap and is not dependent on overall vehicle length.

Gap distributions for each lane are fitted to the observed data for different flow rates in approximately 20 increments up to the maximum observed flow rate in each lane. For each flow rate, three piecewise quadratic curves are fitted to the observed cumulative distributions of gaps up to 4 seconds, in a similar way to that described by OBrien and Caprani [34] for headways. For gaps greater than 4 seconds (in which case following trucks are unlikely to be on the bridge simultaneously), a negative exponential distribution is adopted as a sufficiently accurate approximation. Modifications are made to the gap distributions to account for the observed dependence of gaps on the GVW of each truck, as heavier trucks tend to travel farther apart [35].

The Weibull distribution has been used to model the temporal variation in traffic flows [36] and gives a very good fit for the measured daily traffic volumes. It is used to generate a variable number of trucks for each day of the simulation. It is applied to the slow lane only, and the daily traffic flow in the faster lane is scaled to give the same ratio each day between the flows in the two lanes.

Truck speeds are generated using the empirical frequency distribution for each lane combined

with the method described by Iman and Conover [33] to give the high correlation observed between speeds of successive vehicles. The measurements at the site in the Netherlands are for two same-direction lanes. The simulated traffic is passed in time steps of 0.02 s over simply supported and two-span continuous bridges with lengths ranging from 15 to 30 m in steps of 5 m. Two lanes of traffic are assumed, with traffic in both lanes traveling in the same direction. Maximum load effects are calculated for 3 load effects: i) bending moment (kNm) at mid-span for simply supported span (LE1), ii) shear (kN) at support at entrance to bridge in primary lane, the slow lane which contains the bulk of the truck traffic in same-direction traffic, (LE2) and iii) hogging bending moment (kNm) over the central support of a 2-span continuous bridge (LE3). In each simulation, at least 75 years of traffic is generated, and maximum load effects are calculated for each block of 25 days. For the purposes of comparing simulated and observed results, the bridge is assumed to be a simple beam, and the transverse position of the vehicles is ignored. Traffic growth is accounted for by incorporating daily volume growth corresponding to annual growth rates of 1%, 2%, 3% and 4.1%.

For this analysis, the parameters of the GEV are assumed to vary linearly or quadratically in time:

$$\begin{aligned} \mu(t) &= \alpha_i + \beta_i t + \gamma_i t^2 \\ \sigma(t) &= \delta_i + \varepsilon_i t + \varphi_i t^2 \\ \xi(t) &= \kappa_i + \lambda_i t \end{aligned} \qquad (10)$$

Hence, the parameter vector $\theta(t) = (\mu(t), \sigma(t), \xi(t))$ depends on up to 8 coefficients, α_i, β_i, γ_i, δ_i, ε_i, φ_i, κ_i, and λ_i. The dimensionality of the model is the number of parameters that depend (linear o quadratic) on the covariate t. Parameter estimation in the non-stationary GEV model is generally done using maximum likelihood estimation [37].

In order to determine the best model for growth, 17 different permutations of the 8 possible coefficients are considered for LE1 on a 15 m span bridge with a 4.1% annual traffic growth rate. The combinations considered and the maximum likelihood parameter values are given in Table 1. It is clear from the results that the choice with the highest log likelihood value is No. 17. The nearest alternative choices are Nos. 5, 11, 13 and 15. Of these, Nos. 11, 13 and 15 can be discounted as they have lower log likelihood than No. 17 and the same or higher dimensionality. However, No. 5 is a contender as it has similar log likelihood to No. 17 and lower dimensionality (fewer parameters). Coles [18] describes this principle of parsimony, i.e., seeking the maximum likelihood solution, while minimizing the complexity of the model.

The results summarized in Table 1 confirm the fact that the Gumbel family of distributions is closed under maximization. As the shape parameter derived from the analysis is close to zero, daily maximum distributions are approximately Gumbel. Therefore, the change in traffic daily volume is expected to cause a rightward shift in the original distribution location parameter. Moreover, the scale parameter should stay constant, which is consistent with the small value of $\boldsymbol{\varepsilon}_i$ obtained.

I	α_i	β_i	γ_i	δ_i	ε_i	φ_i	κ_i	λ_i	llh_i	D_i	p_i
1	2.170			0.128			-0.240		307.95	107.28	0
2	2.178			0.125	-0.0214		-0.203		311.52	100.15	1
3	2.169			0.118		0.025	-0.220		309.60	103.99	1
4	2.169	0.094		0.111			-0.156		352.13	18.91	1
5	**2.169**	**0.093**		**0.110**	**-0.025**		**-0.151**		**361.03**	**1.13**	**2**
6	2.169	0.094		0.112		-0.002	-0.157		352.16	18.86	2
7	2.177		-0.021	0.128			-0.239		308.55	106.07	1
8	2.173		0.024	0.124	-0.029		-0.191		311.95	99.27	2
9	2.177		-0.026	0.117		0.026	-0.220		310.47	102.25	2
10	2.179			0.112	-0.029	0.033	-0.174		314.53	94.12	2
11	**2.169**	**0.093**		**0.111**	**-0.024**	**-0.003**	**-0.153**		**361.07**	**1.04**	**3**
12	2.172	0.094	-0.009	0.111			-0.156		352.27	18.64	2
13	**2.170**	**0.093**	**-0.004**	**0.110**	**-0.025**		**-0.151**		**361.06**	**1.06**	**3**
14	2.172	0.094	-0.009	0.112		-0.002	-0.157		352.30	18.59	3
15	**2.173**	**0.094**	**-0.007**	**0.113**	**-0.024**	**-0.005**	**-0.163**		**361.00**	**1.17**	**4**
16	2.173		0.031	0.111	-0.040	0.035	-0.155		315.24	92.70	3
17	**2.169**	**0.089**		**0.110**	**-0.027**		**-0.153**	**0.059**	**361.59**	**0.00**	**3**

Table 1: Maximum Likelihood values for the coefficients (αi, βi, γi, δi, εi, φi, κi, λi) and log-likelihood (llhi), deviance statistics (Di) of each permutation compared with No. 17 and dimensionality of each permutation (pi)

Note: In the table, an empty space implies that this parameter has not been considered. For example, No. 1 is a stationary model with all parameters remaining constant with time and No. 15 allows a quadratic variation of location and scale parameters but constant shape parameter.

To compare two nested models, M_0 and M_i (where it is assumed that $M_i \subset M_0$), Coles [18] uses the deviance statistic:

$$D_i = 2\{l_i(M_i) - l_0(M_0)\} \tag{11}$$

where $l_0(M_0)$ and $l_i(M_i)$ are the maximized log-likelihoods under models M_0 and M_i respectively, and where M_0 is the model with the highest absolute value of log-likelihood. Mathematically, M_i is rejected by a test at the α-level of significance. Thus, if $D > c_\alpha$, M_i is rejected, where c_α is the (1- α) quantile of the χ^2_k distribution and k is the difference in the dimensionalities of M_i and M_0.

In this case, all models are compared to No. 17. No. 5 has a deviance statistic of 1.13. This is tested for significance at the 0.95 level, using a χ^2_k distribution of dimension 1, as there is a unit difference in dimensionality, giving c_α=3.84. On this basis, No. 5 is identified as the best solution, a choice confirmed by the absence of any physical evidence to support a linear change

in the shape parameter.

Therefore, the model adopted for this analysis is expressed as,

$$\mu(t)= \alpha_i+\beta_i \cdot t$$
$$\sigma(t)= \delta_i+\varepsilon_i \cdot t \quad (12)$$
$$\xi(t)= \kappa_i$$

with parameter vector $\theta(t)=(\mu(t),\sigma(t),\xi(t))$ depending on 5 coefficients, α_i, β_i, δ_i, ε_i, and κ_i.

The 5-parameter time-varying model is illustrated in the probability-probability (PP) and quantile-quantile (QQ) plots of Figure 5. The quality of the fits is good, despite some deviation in the tail. While there is considerable deviation in the last few points (out of the total of 750), this is not uncommon in this kind of analysis and is the result of expected random variation in less than 1% of the data.

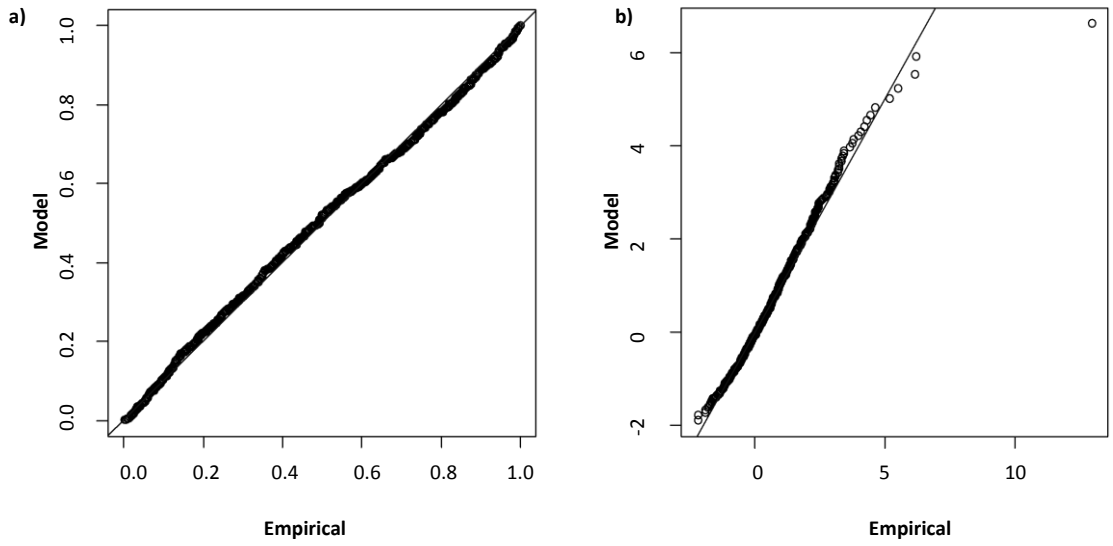

Figure 5: Comparison of 75 years of data for 25-day maximum values of LE1 for 15 m span and growth of 3%. (a) Residual probability plot and (b) Residual quantile plot (Gumbel Scale).

Figure 6 gives results of simulations of LE1 for a 15 m span bridge. The gray points are from the stationary traffic sample and the best fit curve to these points is also shown in gray. The characteristic maximum values for this no-growth situation are 2445 and 2498 kNm for return periods of 20 and 75 years respectively. The points and curve for a 75-year lifetime of growth are shown in black. As there is growth in the number of trucks, there is a general increase in the 25-day-maximum values. The characteristic maximum values are therefore greater at 2544 and 2602 kNm for return periods of 20 and 75 years respectively.

Table 2 gives the errors in the LE values due to the use of the stationary analysis method

instead of the non-stationary one. Values for the non-stationary fit are based on a 75-year lifetime. It can be seen that the stationary assumption is non-conservative but that the resulting errors are relatively small.

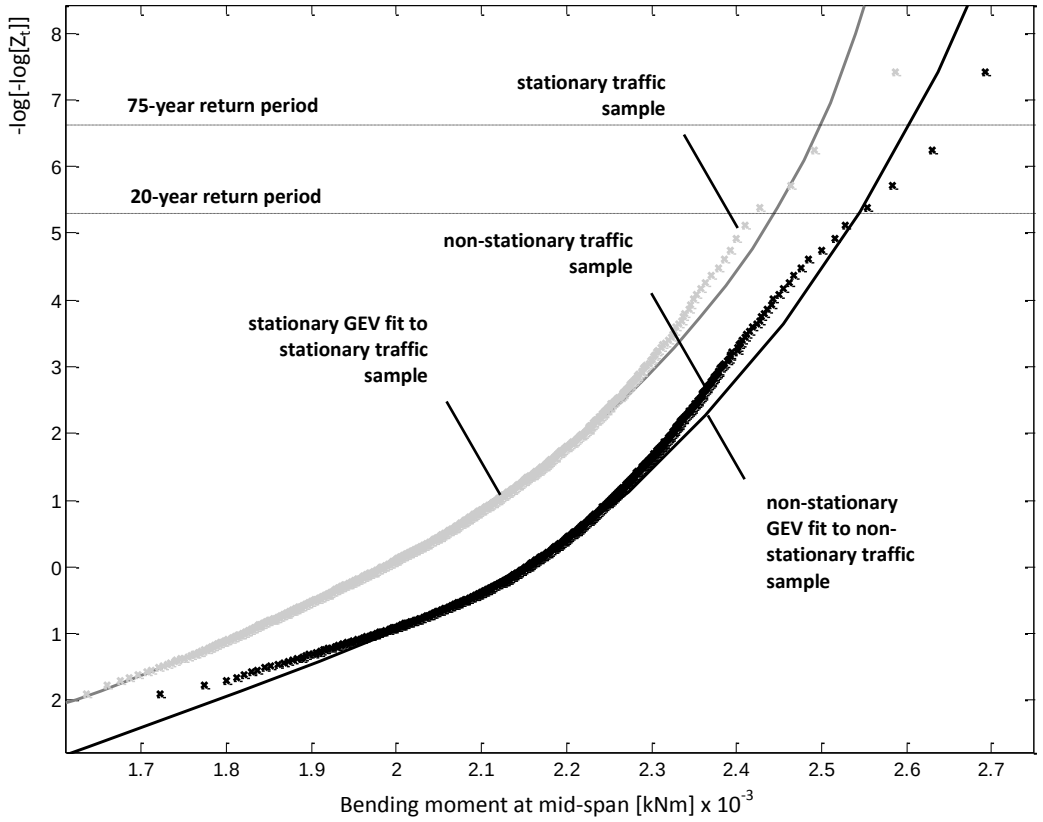

Figure 6: Expected lifetime extreme distributions for LE1 on a 15 m span bridge with 3% annual growth through the 75-year lifetime of the structure.

Table 2: Characteristic load effects and error due to stationary assumption for different return periods and 15 m span bridge.

Load Effect	*Return Period (years)*	*Stationary (No growth)*	*Non-stationary, 75 year lifetime*	*Error in stationary [%]*
LE1 (kNm)	20	2445	2544	-3.9
	75	2498	2602	-4.0
LE2 (kN)	20	702	723	-2.9
	75	714	739	-2.1
LE3 (kNm)	20	679	721	-5.8
	75	691	742	-6.9

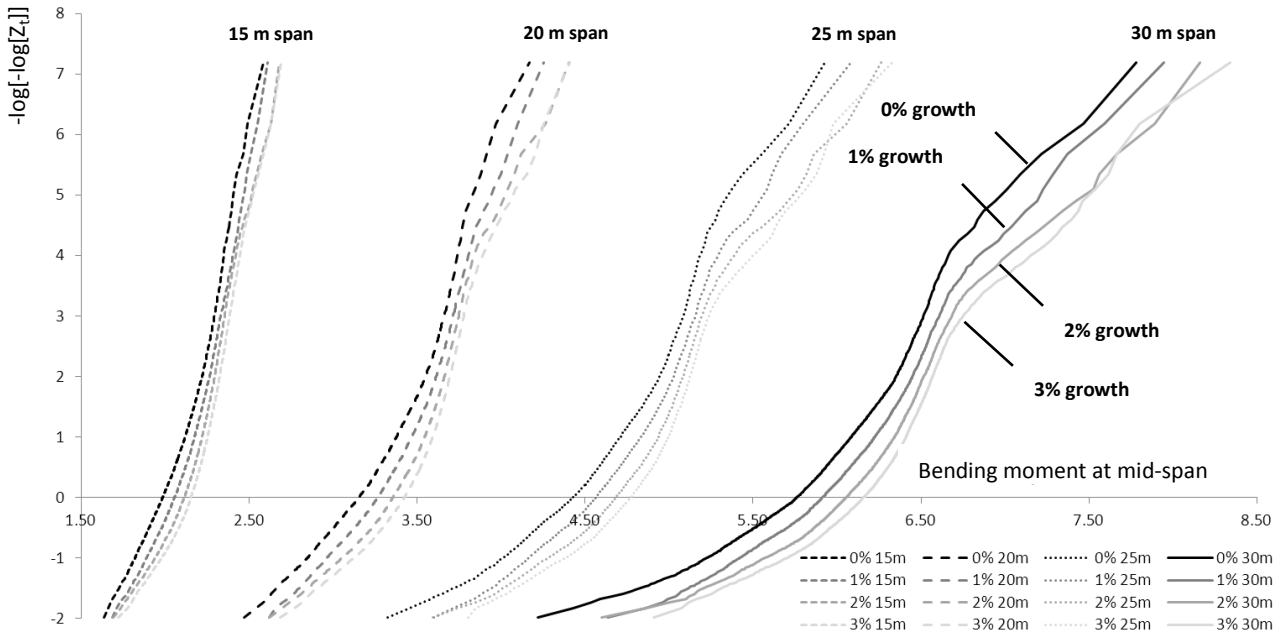

Figure 7: Average results from ten simulations for each span with four different growth rates (0%, 1%, 2%, 3%) over a 75-year lifetime for LE1 (bending moment at mid-span).

LE1 results for all four spans are illustrated in Figure 7. As spans increase, the trend in the upper tails of the curves change slope at higher probabilities of non-exceedance (upper parts of graphs represent rarer events). This suggests that the data comes from a mixed statistical distribution and that a different type of event starts to dominate for rarer events in longer spans. A single fit to all the data in these circumstances is inappropriate [15]. Three types of vehicle can be identified in the 25-day block maxima: i) crane-type vehicle with all axles closely spaced, ii) standard trucks (most vehicles), and iii) low loaders (with a maximum inter-axle spacing greater than 7.5 m). Low loaders are the very heaviest vehicles and, for spans up to 30 m as depicted in Figure 8, the upper tail is composed mainly of load effects that result from this type of vehicle (despite being less frequent). The main body of the distributions is formed by cranes (shorter vehicles). Clearly, for these short span bridges (up to 30m), the effect of heavier low loaders dominates over cranes whose weight is more concentrated.

Data from a mixture of distributions can be partitioned by type into j different sub-samples [15], in this case different vehicle types. The probability that the maximum load effect in the i^{th} event in a given reference period such as a day, S_i, is less than or equal to some value, s, is then given by the Law of Total Probability:

$$P[S \le s] = \sum_{j=1}^{n_t} F_j(s) \cdot f_j \qquad (13)$$

where $F_j(\cdot)$ is the cumulative distribution function for the maximum load effect in a j-type and f_j is the probability of occurrence of that j-type event. The maximum value for all events in the reference period is denoted by S; for example, the maximum-per-25-day load effect in this case.

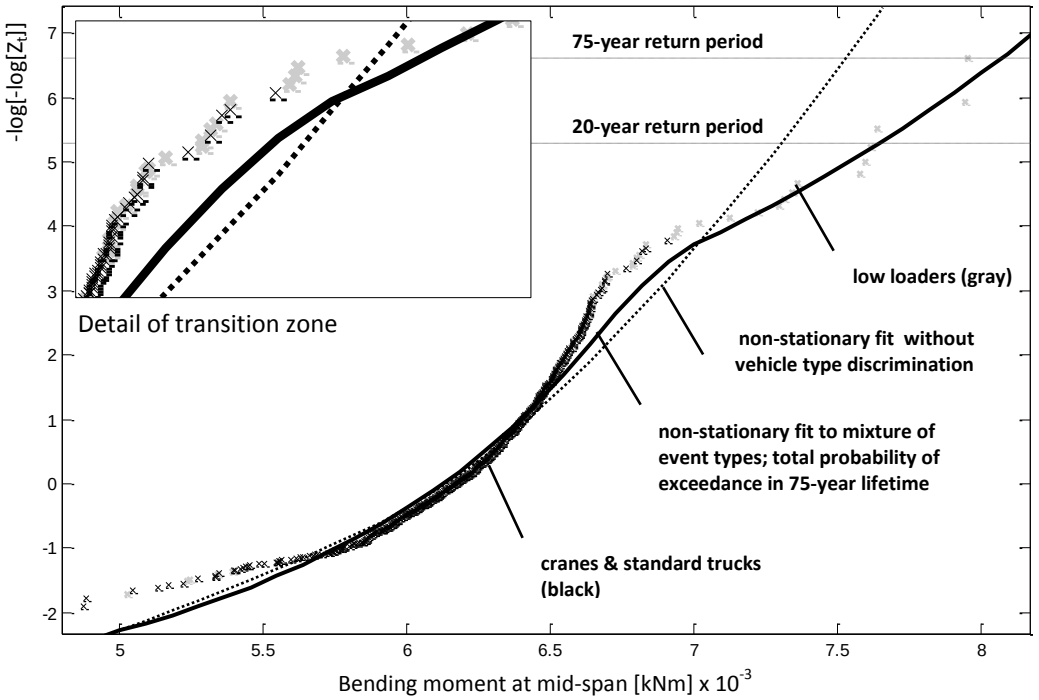

Figure 8: Expected lifetime extreme distributions for LE1 on a 30 m span bridge with 3% annual growth through the 75-year lifetime of the structure. The inset shows the transition zone from predominance of cranes (in black) to low loaders (in gray) around 6700 kNm

For this particular example, on a 30 m span bridge, low loaders were found to govern for 10% of 25-day maxima, with either cranes or standard trucks governing for the remaining 90%. Despite their small number, low loaders dominate at the 20 and 75 year return levels.

Figure 9 gives results of simulations of LE1 for a 30 m span bridge with 3% annual growth. The points are the same as those shown in Figure 8; they all correspond to a 75-year lifetime of growth with the gray representing low-loaders and the black representing other types of vehicle. The 75-year non-stationary best-fit, shown in solid black, is also the same as that shown in Figure 8. For a 20-year lifetime, there are far fewer heavy vehicles and the curve (in gray) is left of the 75-year lifetime curve. Figure 9 also shows a '75-year snapshot' curve (dashed), based on the traffic conditions at the end of the lifetime of the bridge. This is right of the whole lifetime curve as the former has many years in which traffic is lighter.

In general, growth is seen to shift the curve to the right and a longer lifetime of growth results in a greater shift. The characteristic maximum LE's for the 20-year lifetime of growth are 7276 and 7687 kNm for return periods of 20 and 75 years respectively. A 75-year lifetime of growth results in far greater numbers of heavy vehicles in the later years which tend to dominate in many of the 25-day maximum values. The characteristic maximum LE's are therefore greater: 7647 and 8072 kNm for return periods of 20 and 75 years respectively.

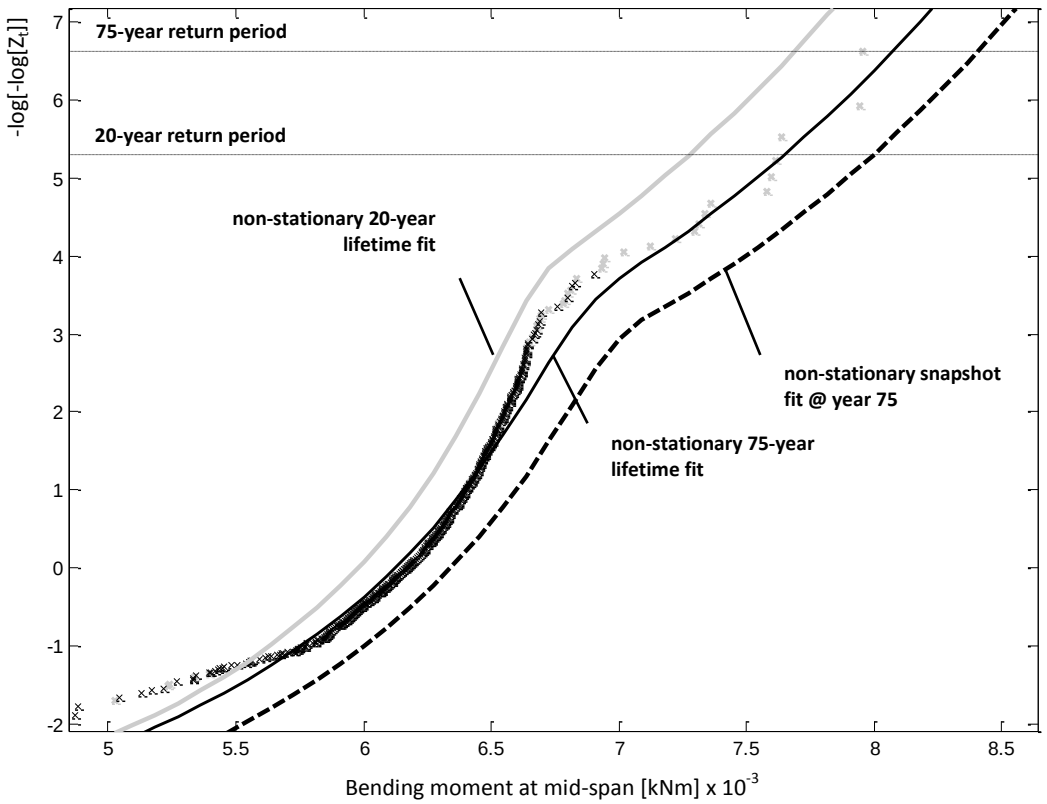

Figure 9: Cumulative distributions for LE1 on a 30 m span bridge with 3% annual growth.

The results are summarized in Table 3. In this case the errors are substantial relative to the non-stationary case with 75 years of growth. Compared to the values obtained for a stationary (no growth) simulation which results in 7136 kNm and 7311 kNm for the 20 and 75-year characteristic values in the example of Figure 9, respectively, the errors are 6.7% and 9.4%.

Table 3: Characteristic load effects and error due to stationary assumption for different return periods and 30 m span bridge.

Load Effect	***Return Period (years)***	***Stationary (no growth)***	***Non-stationary, 20-year lifetime***	***Non-stationary, 75-year lifetime***	***Error of stationary relative to non-stationary with 75-year lifetime [%]***
LE1	20	7136	7276	7647	-6.7
(kNm)	75	7311	7687	8072	-9.4
LE2	20	999	1102	1185	-15.7
(kN)	75	1031	1110	1193	-13.6
LE3	20	974	1026	1047	-7.0
(kNm)	75	1002	1081	1102	-9.1

4. Conclusions

This paper shows the effects of non-stationary traffic data on characteristic maximum traffic load effects. The research has focused on short span brides (up to 30 m) for which free-flowing traffic conditions govern. The results are based on Monte Carlo simulations calibrated with WIM data from a site in the Netherlands. Maximum-per-25-day load effect data is plotted on Gumbel probability paper. For a 15 m span, the trend is uniform, with a single Weibull distribution and growth over 20 years has the effect of increasing the characteristic load effect modestly. For a 30 m span, the trend reflects a mixture of distributions with a change evident as the 25-day maximum values becomes dominated by low loader vehicles in the later years. However, the influence of growth is similar – it generates modest increases in characteristic maximum values.

The difference between lifetime and return period is emphasized, the former being a period with growth while the latter is a measure of safety. The data trend is strongly influenced by the lifetime assumed, with longer lifetimes resulting in greater shifts to the right in the probability paper plots and greater characteristic values.

5. References

[1]. Melchers, R.E., 2001. Assessment of existing structures – Approaches and research needs, Journal of Structural Engineering, 127(4), 406-411.

[2]. Bruls, A., Croce, P., Sanpaolesi, L. and Sedlacek, G., 1996. ENV1991 – Part 3: Traffic Loads on Bridges; Calibration of Load Models for Road Bridges, Proceedings of IABSE Colloquium, Delft, The Netherlands, IABSEAIPC-IVBH, 439-453.

[3]. Flint, A.R. and Jacob, B., 1994. Extreme traffic loads on road bridges and target values for their effects for code calibration, Proceedings of IABSE Colloquium, Delft, The Netherlands, IABSE-AIPC-IVBH, 469-478.

[4]. Nowak, A.S., 1989. Probabilistic basis for bridge design codes, Proceedings of ICOSSAR ’89, the 5th International Conference on Structural Safety and Reliability, San Francisco, Eds A. H.-S. Ang, M. Shinozuka and G. I. Schuëller, ASCE, New York, 2019-2026.

[5]. Nowak, A.S. and Hong, Y.K., 1991. Bridge live load models, Journal of Structural Engineering, ASCE, 117(9), 2757-2767

[6]. Cremona, C., 2001. Optimal extrapolation of traffic load effects, Structural Safety, 23, 31-46.

[7]. Nowak, A.S., 1993. Live load model for highway bridges, Structural Safety, 13, 53-66.

[8]. Fu, G. and Hag-Elsafi, O., 1995. Bridge Evaluation for Overloads Including Frequency of Appearance, Applications of Statistics and Probability, Eds. Favre and Mébarki, Rotterdam, 687-692.

[9]. Ghosn, M. and Moses, F., 1985. Markov renewal model for maximum bridge loading. Journal of Engineering Mechanics. ASCE, 111(9), 1093-1104.

[10]. Crespo-Minguillón, C. and Casas, J.R., 1997. A comprehensive traffic load model for bridge safety checking, Structural Safety, 19, 339-359.

[11]. James, G., 2005. Analysis of traffic load effects on railway bridges using weigh-in-motion data. Fourth International Conference on Weigh-In-Motion (ICWIM4), Eds. E.J. OBrien, B. Jacob, A. González, and C.-P. Chou, National Taiwan University, 351-361.
[12]. Cooper, D.I., 1995. The determination of highway bridge design loading in the United Kingdom from traffic measurements, Pre-Proceedings of the First European Conference on Weigh-in-Motion of Road Vehicles, ed. B. Jacob et al., E.T.H. Zürich, 413-421.
[13]. Cooper, D. I., 1997. Development of short span bridge-specific assessment live loading, Safety of Bridges, ed. P.C. Das, Thomas Telford, 64-89.
[14]. Moyo, P., Brownjohn, J.M. and Omenzetter, P., 2003. Highway bridge live loading assessment and load carrying estimation using a health monitoring system, Proceedings of the 3rd International Conference on Current and Future Trends in Bridge Design, Construction and Maintenance, Eds. B.I.G. Barr et al., Shanghai, China,Thomas Telford, Sep./Oct., 557-564
[15]. Caprani, C.C., OBrien, E.J. and McLachlan, G.J., 2008. Characteristic traffic load effects from a mixture of loading events on short to medium span bridges, Structural Safety, Vol. 30(5), September, 394-404.
[16]. OBrien, E.J. and Enright, B., 2011. Modeling same direction two lane traffic for bridge loading. Structural Safety, 33 (4-5), 296-304.
[17]. European Commission. Directorate General for Energy and Transport, 2008. European Energy and Transport. Trends for 2030. Update 2007.
[18]. Coles, S., 2001. An introduction to statistical modelling of extreme values. Springer. London
[19]. Mendez, F.J., Menendez, M., Luceño, A., Losada, I.J., 2007. Analyzing monthly extreme sea levels with a time-dependent GEV model. Journal of atmospherica and oceanic technology, 24, 894-911.
[20]. Menendez, M. Mendez, F.J., Izaguirre, C., Luceño, A., Losada, I.J., 2009. The influence of seasonality on estimating return values of significant wave height. Coastal Engineering, 56(3), 211-219.
[21]. Stefanakos, C.N. and Athanassoulis, G.A., 2006. Extreme value predictions based on nonstationary time series of wave data. Environmetrics, 17, 25–46.
[22]. Ribereau, P., Guillou, A. and Naveau, P., 2008. Estimating return levels from maxima of non-stationary random sequences using the Generalized PWM method. Nonlinear Processes in Geophysics, 15, 1033-1039.
[23]. Felici, M., Lucarini, V. Speranza, A. Vitolo, R., 2007: Extreme Value Statistics of the Total Energy in an Intermediate-Complexity Model of the Midlatitude Atmospheric Jet. Part II: Trend Detection and Assessment. J. Atmos. Sci., 64, 2159–2175.
[24]. Nadarajah, S., 2005. Extremes of daily rainfall in west central Florida. Climatic Change, 69, 325-342.
[25]. Nogaj, M., Parey, S. and Dacunha-Castelle, D., 2007. Non-stationary extreme models and a climatic application. Nonlinear Processes in Geophysics, 14, 305–316
[26]. Renard, B., Lang, M., Bois, P., 2006. Statistical analysis of extreme events in a non-stationary context via a Bayesian framework: case study with peak-over-threshold data. Stochastic Environmental Research and Risk Assessment 21, 97–112.

[27]. Einmahl and Magnus, 2008. Records in Athletics Through Extreme-Value Theory. Journal of the American Statistical Association, 103(484), 1382-1391.
[28]. Malevergne, Y., Pisarenko, V. and Sornette, D., 2006. On the power of generalized extreme value (GEV) and generalized Pareto distribution (GPD) estimators for empirical distributions of log-returns, Applied Financial Economics, 16(3), 271-289.
[29]. Wang, J., Chaudhury, A. and Rao, H.R., 2008. A Value-at-Risk Approach to Information Security Investment. Information Systems Research, 19(1), 106–120.
[30]. Jenkinson, A.F., 1955. The frequency distribution of the annual maximum (or minimum) of meteorological elements, Quarterly Journal of the Royal Meteorological Society, 81, 158-171.
[31]. Von Mises, R., 1936. La distribution de la plus grande de n valeurs, Revue Mathématique De l'Union Interbalcanique, 1, 141-160. Reproduced in Selected Papers of Richard von Mises, American Mathematical Society, 2, 271-294, Rhode Island, 1964.
[32]. OBrien, E.J., Enright, B. and Getachew, A., 2010. Importance of the Tail in Truck Weight Modeling for Bridge Assessment, Journal of Bridge Engineering, 15(2), 210-213.
[33]. Iman, R.L. and Conover, W.J., 1982. A distribution-free approach to inducing rank correlation among input variables. Communications in Statistics – Simulation and Computation 11 (3), 311 - 34.
[34]. OBrien, E.J. and Caprani, C.C., 2005. Headway modelling for traffic load assessment of short- to medium-span bridges, The Structural Engineer, 83(16), 33-36.
[35]. Harman, D.J. and Davenport, A.G., 1979. A statistical approach to traffic loading on highway bridges, Canadian Journal of Civil Engineering, 6, 494-513.
[36]. Stathopolous, A. and Karlaftis, M., 2001. Temporal and Spatial Variations of Real-Time traffic data in urban areas. Journal of the Transportation Research Board, TRB 1768, 135-140.
[37]. Gilleland, E. and Katz, R.W., 2011. New software to analyze how extremes change over time. Eos, 11 January, 92(2), 13-14.